NOTE: The supplemental materials are organized in reference to, and are meant to be read in parallel with, the manuscript file. Thus, for a particular item of supplemental material, the section headings (e. g., MATERIALS AND METHODS/Treatment) match those of the manuscript file within which reference is made to that item. Each item also has a brief descriptive title (e. g., *Scan Interpretation*).

MATERIALS AND METHODS

Treatment

***Scan Interpretation*.** ^{18}F-FDG PET/CT examinations were interpreted by either of 2 radiologists. The radiologist and project physicist (JB) together reviewed scans using Centricity (GE Healthcare). Non-physiologic regions of elevated intensity relative to immediate surroundings in the ^{18}F-FDG images, and having a corresponding anatomic feature consistent with tumor on CT, were identified as FDG-positive (FDG+) tumors. The axial ranges of such tumors on PET and CT were recorded, and (when measurable) tumor transaxial dimensions were determined on CT by the radiologist. The radiologist designated 1 baseline FDG+ tumor as the target tumor. Target tumor selection was based on PET image intensity and/or size, as well as isolation from adjacent, positively-imaged features.

Follow-up scans were aligned with the baseline scan by automatic, rigid-body coregistration of the CT images. The radiologist determined axial ranges, visualization on PET, and size on CT in the follow-up scans for each of the baseline FDG+ tumors. Tumors not measurable on CT were assessed visually for size change between baseline and follow-up. The radiologist also inspected the follow-up scans for new FDG+ tumors, and the locations of any such tumors were recorded.

***Measurement of ^{18}F-FDG Uptake*.** Tissue uptake was measured in terms of SUL, i. e., lean body mass-normalized activity concentration at time of scan per unit injected activity decay corrected to time of scan (units g/mL). The metric for tumor uptake was SUL_{peak}, defined as the maximum value of SUL averaged within a 1.2 cm diameter sphere scanned over an image volume of interest (VOI) encompassing the tumor. Liver was used as a normal tissue reference. The average (mean SUL) and standard deviation (SD) of voxel SULs within a 3 cm diameter spherical VOI placed in normal-appearing liver parenchyma were determined. At baseline, tumors with $SUL_{peak} \geq 1.5$ x (mean SUL + 2 SD) were considered potentially measurable for uptake of ^{18}F-FDG.

Measurements of ^{18}F-FDG uptake in liver and tumors were performed by the project physicist using XD (version 3.6; Mirada Medical). For a given tumor, the baseline scan was inspected for apparent misalignment of PET and CT tumor images, and any such errors were corrected by manual, rigid body registration. A 3-dimensional rectangular VOI (threshold setting = 0% of maximum) containing the tumor image as identified by the radiologist was then defined. Once a VOI was defined, the software automatically indicated the location of the maximum voxel. The size and location of the rectangular VOI were adjusted as needed to bring the maximum voxel within the tumor CT image, and the threshold was set such that the isocontour approximated the boundary of the tumor on CT. {This procedure is a variant of maximum voxel-based thresholding [MVBT (*1*)].} The PET images were inspected to determine whether the tumor image was overlapped by a positively-imaged adjacent feature. If not, uptake was equated with SUL_{peak} automatically calculated for the tumor VOI, and it was noted whether or not uptake exceeded the PERCIST threshold for measurability. All target tumors were measurable for uptake at baseline. In one instance, 2 spatially-separated FDG+ tumors within the thoracic spine were treated as a single tumor. That VOI comprised 2 discontiguous axial segments, with the maximum voxel for each segment lying within the tumor CT image. The largest value of SUL_{peak} for the combined segments was recorded.

Quantitative analysis of follow-up ^{18}F-FDG PET/CT examinations began with automatic, rigid-body coregistration of the follow-up and baseline CT scans. For a given baseline-measurable

tumor, axial alignment was adjusted to maximize similarity between the follow-up and baseline CT images of the tumor and adjacent anatomy. If needed, the PET image of the tumor was manually realigned with the CT image. The tumor region within the follow-up PET scan was then segmented by the MVBT technique, with threshold adjusted such that the volume of the VOI approximated that of the tumor's VOI in the baseline scan. In the absence of evident overlap with adjacent PET-positive features, SUL_{peak} was recorded for the follow-up scan.

Categorization of Response. Response assessment adhered to PERCIST. ^{18}F-FDG PET/CT examinations were interpreted by either of 2 radiologists (LT, NG), blinded to the ^{64}Cu-DOTA-trastuzumab PET/CT examinations. Tumors were measurable if SUL_{peak} was $\geq$ 1.5 x (mean SUL + 2 standard deviations) in normal-appearing liver. For individual tumors, positive "metabolic response" between baseline and follow-up was defined as $\geq$ 30% and 0.8 SUL unit decrease in SUL_{peak}, with $\leq$ 30% increase in tumor size on CT. Tumor progression was defined as $\geq$ 30% and 0.8 SUL unit increase in SUL_{peak}, and/or visible increase in the spatial extent of ^{18}F-FDG uptake with no decline in SUL_{peak}. Assessment of patient response centered on the target tumor. Positive response at the patient level required positive response by the target tumor, non-progression of all non-target, FDG+ tumors identified at baseline, and no new FDG-avid tumors typical of cancer and not infection or treatment effect. Patient progression was defined as progression of 1 or more FDG+ tumors identified at baseline, and/or detection at follow-up of 1 or more new FDG+ tumors.

^{64}Cu-DOTA-trastuzumab PET/CT Image Analysis

***Interpretation of ^{64}Cu-DOTA-trastuzumab PET/CT scans*.** ^{64}Cu-DOTA-trastuzumab PET/CT scans were interpreted by an expert radiologist (JP) different from those who evaluated the ^{18}F-FDG PET/CT examinations. For all patients, interpretation and quantitative analysis of the ^{64}Cu-DOTA-trastuzumab PET/CT scans was performed before follow-up ^{18}F-FDG PET/CT examinations. The radiologist and project physicist jointly reviewed scans via Centricity. Analysis was limited to tumors measureable for baseline ^{18}F-FDG uptake and fully included in the ^{64}Cu-DOTA-trastuzumab PET/CT scans. Tumors for which the ^{64}Cu images extended into the final 2 slices at either end of the axial field of view (FOV), where random noise tends to be excessive, were excluded. ^{64}Cu-DOTA-trastuzumab and baseline ^{18}F-FDG PET/CT scans were aligned by automatic, rigid-body coregistration of the CT images and displayed side-by-side. Axial alignment was adjusted tumor-by-tumor to maximize visual similarity of the CT images. The radiologist then identified the axial ranges of the tumor images in the ^{64}Cu-DOTA-trastuzumab PET/CT scans.

***Measurement of ^{64}Cu-DOTA-trastuzumab Uptake*.** Quantitative analysis of ^{64}Cu-DOTA-trastuzumab scans was performed by the project physicist using XD, version 3.6. Importantly, VOIs and coregistered scans could be saved for subsequent review and editing, and scan coregistration was manually adjustable in 3 dimensions. Tumor uptake was measured in terms of maximum voxel standardized uptake value, $SUV_{max.}$ Once a VOI was defined, the software automatically indicated the location of the maximum voxel and calculated SUV_{max}. No more than 10 tumors were evaluated per patient.

Measurement of tumor uptake began with automatic, rigid-body coregistration of the CT scans for the baseline ^{18}F-FDG and ^{64}Cu-DOTA-trastuzumab examinations. The various PET and CT scans were displayed side-by-side in transaxial mode. For a given tumor and ^{64}Cu-DOTA-trastuzumab PET/CT scan (day 1 or 2), axial alignment was manually adjusted to maximize visual similarity of the CT images of the tumor and adjacent anatomy with those in the ^{18}F-FDG PET/CT scan. The scans were inspected for misalignment of PET and CT tumor images, and any such errors were corrected by manual, rigid-body registration. The ^{64}Cu-DOTA-trastuzumab scan was then inspected within the tumor region as identified by the radiologist. If the tumor image was obscured by an adjacent, positively-imaged feature (as in Supplemental Fig. 1A), the image was rejected for uptake measurement. If the tumor image was positive relative to its surroundings and

well separated from images of adjacent features, the tumor image was segmented by the MVBT technique and evaluated for SUV_{max} via a procedure analogous to that described for ^{18}F-FDG (Supplemental Fig. 1B). In some cases, the rectangular VOI could not be adjusted to bring the maximum voxel within the tumor CT image while simultaneously encompassing the entire ^{64}Cu tumor image. For those tumors, the VOI was divided into 2 or more contiguous axial segments which together included the entire tumor PET image, and for which the maximum voxel for each segment lay within the tumor CT image. The largest value of SUV_{max} for the combined segments was recorded. For the tumor with the 2-segment, axially discontiguous FDG VOI, the ^{64}Cu-DOTA-trastuzumab VOIs analogously comprised 2 axially-discontiguous segments.

Instances in which the influence of positive adjacent features was equivocal required a more careful approach, as illustrated in Supplemental Fig. 1C. Analysis of the day 1 and 2 tumor images was performed simultaneously when both were available. Any evident PET-CT misalignment was corrected. Full, 3-dimensional (3-D) coregistration of tumor images from the FDG and trastuzumab scans was then accomplished by manually adjusting the initial, approximate alignment of the CT scans. Comparison of tumor to background contrast between days 1 and 2 helped identify the locus of tumor uptake. Next, the ^{64}Cu scans were segmented within the tumor region via the MVBT technique, and the maximum intensity voxels were identified. The location of the ^{18}F-FDG tumor VOI was traced within the ^{64}Cu-DOTA-trastuzumab scans using coregistered crosshairs displayed simultaneously on the ^{18}F and ^{64}Cu images. For a given ^{64}Cu-DOTA-trastuzumab image, the SUV_{max} measurement was accepted if the maximum voxel appeared to be associated with tumor and not overlapped by the PET-positive image of an adjacent feature.

Some ^{64}Cu-DOTA-trastuzumab tumor images could not be segmented by the MVBT technique because of low or negative contrast relative to adjacent features (Supplemental Fig. 1D). In those instances, the ^{18}F-FDG VOI was “projected”, i. e., copied, voxel-by-voxel onto the coregistered ^{64}Cu image set. The procedure employed correction of PET-CT misalignment when needed, as well as full, 3-D coregistration of tumor CT images from different scans. The coregistered crosshairs were used to guide VOI voxel selection in the ^{64}Cu images. When a ^{64}Cu VOI was completed, its maximum voxel was identified and evaluated both for association with the CT correlate and overlap by adjacent PET-positive features. If the tumor was deemed measurable, SUV_{max} was recorded.

Statistical Plan and Analysis

The study was designed to accrue 10 patients to explore the relationship between tumor uptake of ^{64}Cu-DOTA-trastuzumab as measured by PET/CT and tumor response to T-DM1 as assessed by ^{18}F-FDG PET/CT. For individual tumors, a hierarchical (tumor-within-patient) linear mixed-effects model was used to evaluate the association between day 1 or day 2 SUV_{max} and PERCIST response. We also identified the best SUV_{max} cutpoints for distinguishing between responsive and non-responsive tumors assuming individual tumor response was determined by uptake and not related to patient. Days 1 and 2 were considered independently. Optimal cutpoints (response thresholds) for individual tumors were used in patient-level categorical analysis [intra-patient average or minimum tumor SUV_{max} > response threshold yes/no vs responsive yes/no; Fisher’s exact test (2-sided *P* values reported)]. Planned comparisons of average uptake in responsive vs non-responsive patients employed the t-test (means and 2-sided *P*-values reported). Survival analysis used Cox Regression to compare patient-level tumor uptake of ^{64}Cu-DOTA-trastuzumab with TTF. Time to treatment failure was the time from start of TDM1 therapy until progression, death or other reasons for treatment discontinuation. Calculations were performed with R version 3.2.1 (R Foundation for Statistical Computing) and StatXact-12 (Cytel Studio).

RESULTS

Patients and Treatment

Qualifying Biopsy and Histopathology. Referencing supplemental Table 1, the patient with IHC score = 1+ was, due to the aggressiveness of her disease, also evaluated by FISH and found to be HER2-positive (HER2+).

HER2+ distant metastasis was verified within 2 mo prior to study entry for 8 of the 10 patients. Of the 2 patients not retested, one was considered for study 4 mo after surgical resection of disease recurrence in brain that was determined to be HER2+. The tumor bed was subsequently ablated with external-beam radiation and hence was not available for reevaluation of HER2 status. The patient had a long history of HER2-negative metastatic disease and presented with multiple somatic tumors. She was included in the study based on the possibility that 1 or more of those tumors was HER2+. As it turned out, the patient had a metabolic partial response to T-DM1. The other patient not retested was included in the study based on HER2+ biopsy/histopathology 7 mo prior to her ^{64}Cu-DOTA-trastuzumab PET/CT examination. That patient had received no anti-HER2 treatment after the biopsy, and hence was accepted for study without reassessment of HER2 status.

***Timing and dosage for T-DM1 administrations*.** Nine patients received their first dose of T-DM1 on day 2, following completion of the ^{64}Cu-DOTA-trastuzumab PET/CT scan. Eight of those were given the standard regimen (3.6 mg/kg every 3 wk), while 1 required a reduced dosage of 2.7 mg/kg. One additional patient began treatment 9 d after injection of ^{64}Cu-DOTA-trastuzumab; she received 2.7 mg/kg for the first 2 tri-weekly administrations and 3.0 mg/kg thereafter.

Patient Outcome

***^{18}F-FDG PET/CT Scans*.** For 1 patient, the ^{18}F-FDG PET/CT baseline examination was obtained with an Optima 560 PET/CT scanner (GE Healthcare) instead of the Discovery STe 16 scanner. That patient failed treatment before her first follow-up FDG examination, so differences between the two scanners did not affect comparison between ^{64}Cu-DOTA-trastuzumab PET/CT results and response to T-DM1.

Timing of ^{18}F-FDG PET/CT Examinations and Number of Follow-up Examinations per Patient. Baseline ^{18}F-FDG PET/CT scans were acquired prior to initiation of T-DM1 therapy [3-23 d (median 7 d)], except for 1 patient for whom the scan could not be obtained until 3 d after the first T-DM1 dose. In the latter case, the (diabetic) patient was hyperglycemic at the intended time of the baseline FDG examination, 1 d prior to the scheduled preparation and injection of ^{64}Cu-DOTA-trastuzumab and 3 d prior to the scheduled first T-DM1 dose. Two patients failed treatment before any follow-up ^{18}F-FDG PET/CT. The other 8 had their first FDG follow-up scans after 2 (n = 7) or 3 cycles of T-DM1, and 6 of those had at least 1 additional follow-up scan.

Adherence to PERCIST-Prescribed Quality Assurance. All patients had serum glucose concentration < 200 mg/dL, and none were receiving insulin. Injected activity (A_{inj}; range 348-559 MBq, median 485 MBq) differed ≤ 20% between baseline and follow-up scans, except in 1 instance, where a follow-up exceeded baseline by 26%. In that case, however, observed tumor response was dramatic (complete disappearance) and clearly not the result of different noise levels in the baseline and follow-up images secondary to the difference in A_{inj}. Time between injection and scan (t_{scan} - t_{inj}) ranged from 56-72 min (median 63 min), except for 1 patient, for whom a scheduling conflict caused baseline (and hence follow-up) t_{scan} - t_{inj} to range from 114-122 min. In all instances, t_{scan} - t_{inj} varied < 15 min between baseline and follow-up scans.

***Correction for Altered ^{18}F-FDG Biodistribution Between Baseline and Follow-up Examinations*.** The patient in question had severe pericardial tamponade at the time of the baseline scan (Supplemental Fig. 2). Blood clearance of ^{18}F-FDG was abnormally slow and liver uptake abnormally high in that examination compared with follow-up scans for that patient, as well as ^{18}F-FDG PET/CT examinations for other patients included in the study. At follow-up, the tamponade had resolved, and tumor to non-tumor contrast was markedly decreased (Supplemental Fig. 2). We assumed that tumor uptake in the baseline examination was increased in proportion to the observed increase in liver uptake (both increases resulting from increased exposure to circulating ^{18}F-FDG), and so calculated percent changes in tumor SUL_{peak} ($\%\Delta SUL_{peak}$) between baseline (bl) and follow-up (fu) as

$$\%\Delta SUL_{peak} = 100\{[SUL_{peak}(fu) \times SUL_{mean}(bl)/SUL_{mean}(fu)]/SUL_{peak}(bl) - 1\} \ ,$$

where SUL_{mean} is average uptake measured in liver. Three tumors had baseline uptake above threshold for measurability. Even with the correction, all 3 showed > 40% reduction in uptake at follow-up and so were classified as having responded positively to T-DM1.

Individual Tumor Response

Tumor Response Measurements vs. Baseline-Measurable Tumors. Fifty-nine tumors, including all 10 target tumors, were measurable for FDG uptake at baseline. The 2 patients without follow-up FDG examinations had a combined total of 12 measurable tumors. Follow-up measurements were rejected for 1 baseline-measurable tumor, a brain metastasis that had recurred following surgical resection, because the tumor image was obscured by increased uptake in adjacent brain in the follow-up scans. Thus, response was measured for 46 tumors. Target tumor response was measured for all 8 patients who had follow-up FDG examinations.

^{64}Cu-DOTA-trastuzumab Imaging

***Scan Acquisitions*.** All patients underwent ^{64}Cu-DOTA-trastuzumab PET/CT scans during the 1st and 2nd days after injection of the radiolabeled antibody (injected activity 475-606 MBq, median 546 MBq). Day 1 and 2 scans began, respectively, 16-28 h (median 24 h) and 39-49 h (median 44 h) post injection.

***Correction of Tumor Uptake Measurements for ^{64}Cu-DOTA-trastuzumab Scans Acquired as ^{18}F*.** For 2 patients, the day 1 ^{64}Cu PET scans were inadvertently acquired as ^{18}F scans. Because list mode data were not retained, the scans could not be reconstructed remedially as ^{64}Cu. Counts recorded during a PET scan are individually corrected for radioactive decay during the scan. For that reason, the error could not be fully corrected simply by accounting for differences between ^{64}Cu and ^{18}F in positron branching ratio and radioactive decay between injection and scan.

For a scan that begins at time t_{sc}, SUV is defined as

$$SUV = AC(t_{sc})\, W_b / [D_{inj} \exp(-\lambda(t_{sc} - t_{inj})] \quad , \qquad (8)$$

where $AC(t_{sc})$ is the activity concentration in the volume of interest (VOI, e. g., a tumor), W_b is the patient's body weight, D_{inj} is the activity injected at time t_{inj}, and λ is the decay constant for the injected radioisotope. $AC(t_{sc})$ is determined from the spatial density of counts acquired from the VOI. The decay-corrected count density for a VOI included within a PET scan's i^{th} bed position can be written as

$$t_{sc}+i\Delta t$$

$$C(i) = S \times BR \int_{t_{sc}+(i-1)\Delta t} dt\, AC(t) \exp[\lambda(t-t_{sc})] \quad , \qquad (11)$$

where S represents the scanner detection sensitivity, BR is the positron branching ratio for the specified radioisotope, Δt is per-bed scan duration, and $\exp[\lambda(t-t_{sc})]$ is the intra-scan decay correction factor. Specializing to the case of ^{64}Cu-DOTA-trastuzumab, activity concentration can be written as

$$AC(t) = AC(t_{sc})\exp[-\lambda(^{64}Cu)(t-t_{sc})] \quad ,$$

where $\lambda(^{64}Cu)$ is the decay constant for ^{64}Cu. When the scan is correctly acquired as ^{64}Cu, evaluation of the integral in Eq. 2 gives

$$C(i, ^{64}Cu) = S \times BR(^{64}Cu) \times AC(t_{sc}) \times \Delta t \quad . \qquad (12)$$

When the scan is acquired as ^{18}F, C(i) becomes

$$C(i, ^{18}F) = S \times BR(^{18}F) \times AC(t_{sc}) \times \exp\{\lambda(^{18}F\text{-}^{64}Cu)i\Delta t\} \times \{1 - \exp[-\lambda(^{18}F\text{-}^{64}Cu)]\}/ \lambda(^{18}F\text{-}^{64}Cu) \quad ,$$

where $\lambda(^{18}F\text{-}^{64}Cu) = \lambda(^{18}F) - \lambda(^{64}Cu)$.

Using Eqs. 1, 3 and 4, we derived the following SUV correction factor CF for a VOI included in bed position i of a scan incorrectly acquired as ^{18}F instead of ^{64}Cu:

$$CF(i,^{18}F \rightarrow {}^{64}Cu) = \exp\{[\lambda(^{64}Cu) - \lambda(^{18}F)][t_{sc} - t_{inj}]\} \times [BR(^{18}F)/BR(^{64}Cu)] \times \exp\{[\lambda(^{64}Cu) - \lambda(^{18}F)][i-1/2)\Delta t]\} \quad .$$

Note that the first factor corrects the error in the adjustment of D_{inj} for radioactive decay between injection and scan, while the third factor corrects the error in the intra-scan decay correction. The correction factor is exact, except that it does not account for the randomness of radiodecay during the scan acquisition.

***Tumor Uptake Measurements*.** Utilization of the various methods of image alignment, tumor image segmentation and assessment of SUV_{max} measurability is summarized in Supplemental Table 2. Full 3-D coregistration was required for about ½ of the evaluated tumors, and approximately ¼ of the tumors required correction of PET-CT alignment for at least 1 of the 3 scans (FDG baseline, day 1, day 2). Most of the tumor images were segmented via the MVBT technique, and measurability was assessable by visual inspection for about ½ of the tumor images. Approximately ¾ of the tumor images were judged to be measurable for SUV_{max}.

Supplemental Table 3 shows for each patient the number of tumors measured for response, ^{64}Cu-DOTA-trastuzumab SUV_{max} and both response and ^{64}Cu-DOTA-trastuzumab SUV_{max}. As noted in the manuscript file, 1 patient's day 2 scan included no baseline FDG-measurable tumors, and hence no tumors were measured for ^{64}Cu-DOTA-trastuzumab uptake in that scan. The limit of 10 SUV_{max} measurements was reached in the day 1 scans for 2 patients.

DISCUSSION

***Estimation of ^{64}Cu-DOTA-Trastuzumab Blood SUV and Tumor SUV_{max} T-DM1 Response Threshold at 4 d Post Injection*.** We determined ^{64}Cu-DOTA-trastuzumab blood pool SUVs at 1 and 2 days post injection via PET image analysis and direct measurements performed on

peripheral venous blood samples drawn before imaging on days 1 and 2. Individual PET-derived SUV measurements were voxel averages over image VOIs. Blood pool VOIs excluded the first 2 and last 2 transaxial slices of a given scan, which are prone to excessive random noise. For day 1, 3-D VOIs (threshold setting = 50% of maximum) were defined which encompassed the mediastinum from the proximal surface of the aortic arch through the distal surface of the heart (Supplemental Fig. 3A). The VOIs were edited to remove small vessels and features not representing blood pool. Thresholding and editing of day 2 VOIs were performed to maximize visual similarity of isocontours with those of the corresponding day 1 VOIs. Day 2 scans fully and partially included the mediastinum for 4 and 5 patients, respectively, and completely excluded the mediastinum for 1 patient. For the latter patient, day 2 blood pool SUV was computed as scan-derived day 1 blood pool SUV x the ratio of day 2 to day 1 blood activity concentration determined by venous sampling. For the other 9 patients, day 2-to-day 1 ratios of image-derived blood SUVs were verified by comparison with direct measurements. On average, the two data sets agreed within 2% (range -13 to +5%).

Estimation of ^{64}Cu-DOTA-trastuzumab blood pool SUV at 4 d (96 h) post injection employed trastuzumab blood clearance curves determined in studies with ^{89}Zr-trastuzumab. Laforest, et al., reported monoexponential blood clearance [half-life ($t_{1/2}$) = 113 h] of ^{89}Zr-trastuzumab between 1 and 6 d post injection in women with HER2+ breast cancer (*2*). O'Donoghue, et al., had a very similar finding ($t_{1/2}$ = 111 h) between 1 and 8 d post injection in patients with esophagogastric cancer (*3*). We estimated ^{64}Cu-DOTA-trastuzumab blood pool SUV at 96 h by normalizing (least-squares best fit) a monoexponentially decaying curve ($t_{1/2}$ = 112 h) to inter-patient (n = 10) average blood pool SUV at 1 and 2 d post injection in our study (Supplemental Fig. 3B).

The uptake threshold for tumor response at 96 h was estimated using measurements of tumor uptake of ^{89}Zr-trastuzumab vs time reported by O'Donoghue, et al., (*3)* in relation to our determinations of response thresholds for ^{64}Cu-DOTA-trastuzumab uptake at 1 and 2 d post injection. Uptake data for ^{89}Zr-trastuzumab at 2, 24, 48 and 120 h post injection were estimated from O'Donoghue, et al., Fig. 2 and fitted with a 1-phase exponential association curve [$a + b(1-e^{-ct})$]. The fitted curve was then normalized (least-squares best fit) to our determinations of ^{64}Cu-DOTA-trastuzumab tumor SUV_{max} response thresholds on days 1 and 2 and evaluated at 96 h (Supplemental Fig. 3B).

Estimated blood pool SUV and SUV_{max} response threshold at 96 h are 5.0 and 6.5 g/mL, respectively (Supplemental Fig. 3B).

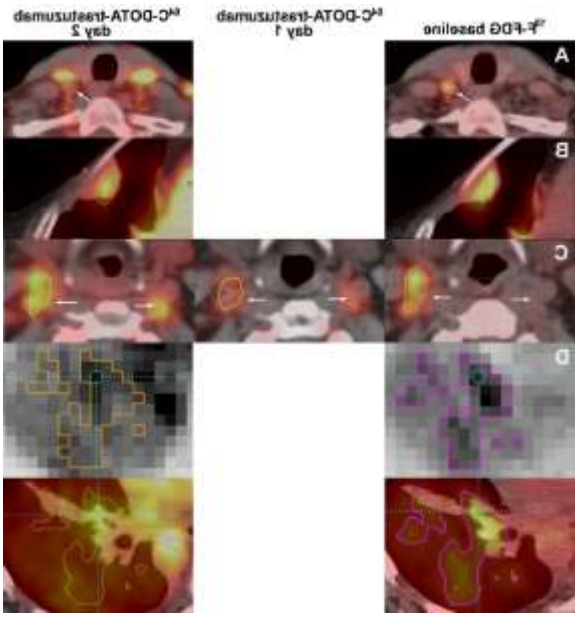

SUPPLEMENTAL FIGURE 1. Measurement of 64Cu-DOTA-trastuzumab uptake in tumors. Except for the top row of part D, the images (single transaxial slices) are smoothed PET (color) -CT fusions. For the PET images, black corresponds to SUV = 0 g/mL. Tumor image alignment is optimized in the axial dimension for A and B, and in 3 dimensions for C and D. **(A)** Measurements were rejected for this metastatic left cervical node (arrows) because 64Cu images of the tumor were strongly overlapped by images of adjacent blood vessels. Maximum intensity (white) corresponds to SUV = 5 g/mL for both 18F-FDG and 64Cu-DOTA-trastuzumab. **(B)** This left chest wall metastasis was well isolated from other positively imaged features. Maximum voxel-based thresholding (MVBT) was applied. The isocontour shown for FDG corresponds to a 50% threshold, while that for 64Cu-DOTA-trastuzumab is for a VOI with volume equal to that of the FDG VOI. Maximum intensity (white) corresponds to SUV = 5 g/mL for both 18F-FDG and 64Cu-DOTA-trastuzumab. **(C)** Adjacent blood vessels (right- and left-pointing arrows indicate ipsilateral and contralateral vessels, respectively) might have influenced measurement of 64Cu uptake in this metastatic left cervical nodal conglomerate. Tumor delineation was facilitated by increased tumor-to-background contrast on day 2. Maximum PET image intensity (white) corresponds to SUV = 10 g/mL for all 3 images. Isocontours correspond to 50% threshold for FDG and FDG volume-matched VOIs for trastuzumab. Crosshairs for FDG and day 2 are centered on the day 2 maximum voxel, while that for day 1 is centered on the day 1 maximum voxel. SUVmax measurement was rejected for day 1 due to likely overlap with the vessel image and accepted for day 2 because the maximum voxel was well isolated from the vessel image. **(D)** Low tumor-to-background contrast precluded MVBT segmentation of the 64Cu images for this malignant region in the patient's left lung. The top row shows non-smoothed PET gray scale images with the FDG MVBT 50% threshold isocontour and its voxel-by-voxel projection onto the coregistered day 2 scan superimposed. Differences between the two isocontours reflect spatial offset of voxel centers between the coregistered scans. Maximum intensity (black) corresponds to SUV = 5 and 7 g/mL for 18F-FDG and 64Cu-DOTA-trastuzumab, respectively. The bottom row shows the corresponding, smoothed images and isocontours. Crosshairs are centered on the day 2 maximum voxel. For the PET images, maximum intensity (white) corresponds to SUV = 5 and 7 g/mL for 18F-FDG and 64Cu-DOTA-trastuzumab, respectively. MVBT = maximum voxel-based thresholding; VOI = volume of interest; SUV = standardized uptake value (activity concentration decay-corrected to time of injection x body weight ÷ injected activity); SUVmax = single-voxel maximum SUV.

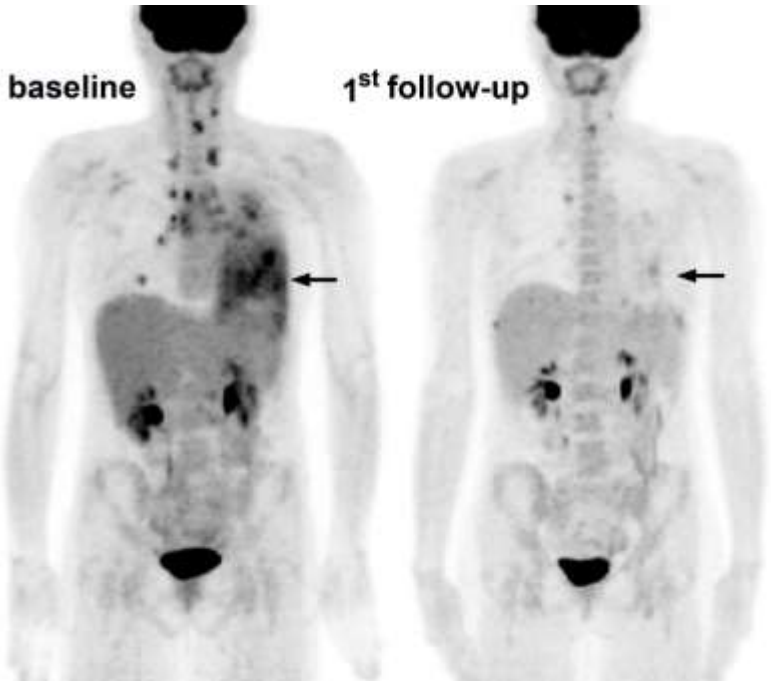

SUPPLEMENTAL FIGURE 2. Correction for altered ^{18}F-FDG biodistribution between baseline and follow-up examinations. Images are maximum intensity projections. Minimum (white) and maximum (black) intensities correspond to SUL = 0.0 and 5.6 g/mL, respectively. Severe pericardial tamponade evident at baseline was resolved at first follow-up (arrows), conducted 2 mo later after 2 cycles of T-DM1. Liver SUL was 2.3 g/mL at baseline and 1.3 g/mL at follow-up. Tumor-to-background contrast decreased markedly in the follow-up, and, despite upward correction of follow-up tumor uptake values for the altered biodistribution, the patient was classified as having partial metabolic response according to PERCIST. The apparent new lesion at the right hepatic periphery seen at 1st follow-up reflects focal uptake in a rib, which was below the PERCIST threshold for measurability and resolved at 2nd FDG follow-up. SUL = lean body mass-normalized standardized uptake value (activity concentration decay-corrected to time of injection x lean body mass ÷ injected activity).

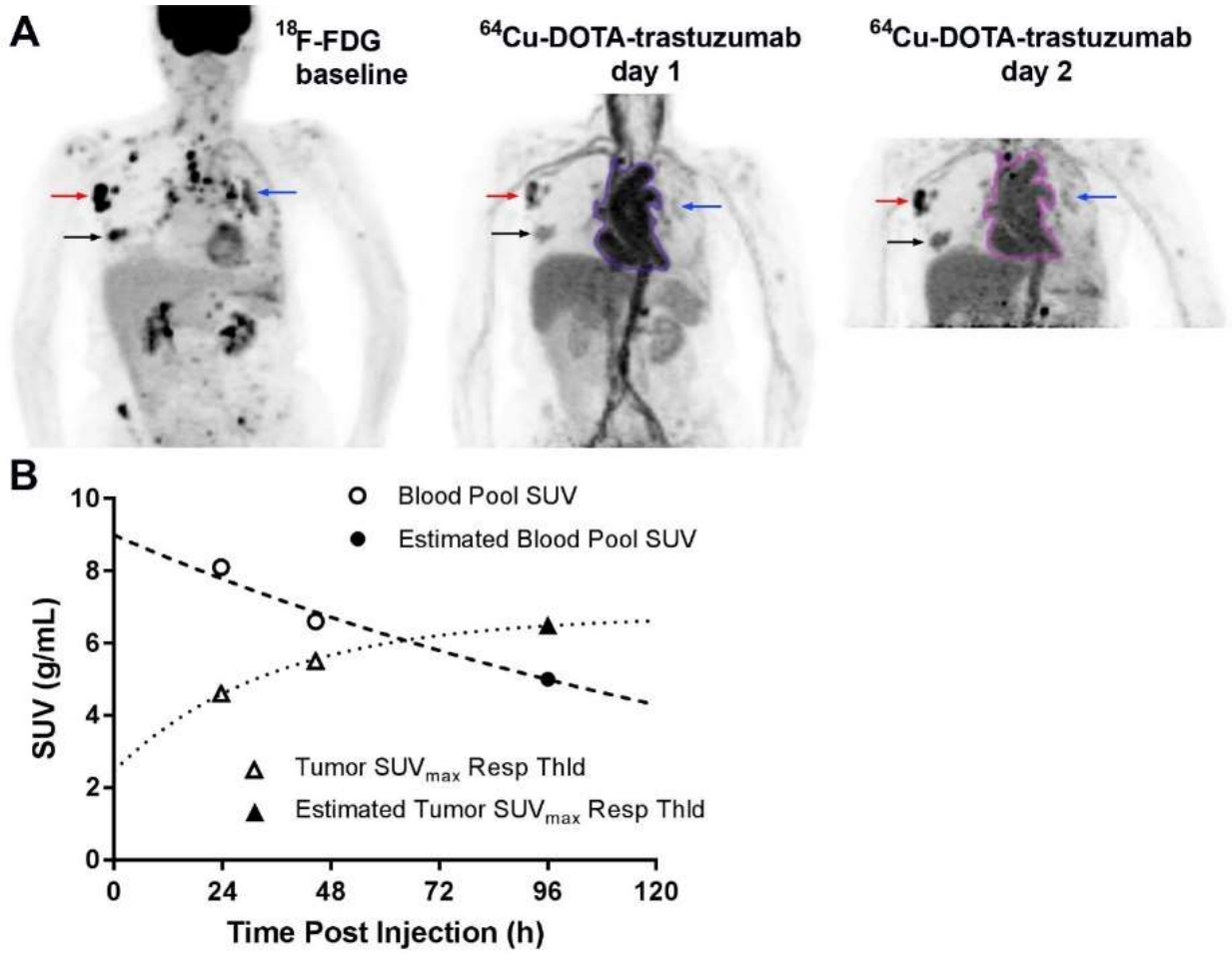

SUPPLEMENTAL FIGURE 3. Estimation of ^{64}Cu-DOTA-trastuzumab blood SUV and tumor SUV_{max} T-DM1 response threshold at 4 d post injection. **(A)** Comparison of maximum intensity projection (MIP) images for a patient with highly variable ^{64}Cu-DOTA-trastuzumab uptake among different FDG-positive tumors. Red, black and blue arrows respectively identify tumors with ^{64}Cu uptake well above, modestly above and modestly below the response threshold. Blood pool volume-of-interest (VOI) boundaries are outlined in purple (day 1) and magenta (day 2). Minimum intensity (white) corresponds to SUV = 0 g/mL. Maximum intensity (black) corresponds to SUV = 7 and 10 g/mL for ^{18}F-FDG and ^{64}Cu-DOTA-trastuzumab, respectively. **(B)** Extrapolation to 4 d post injection. Blood pool SUV data (open circles) are VOI mean SUVs averaged over the 10 patients included in this study. Dashed line: trastuzumab blood clearance curve [$t_{1/2}$ = 112 h (*2, 3)*] normalized to the patient-averaged day 1 and 2 blood pool SUVs. Dotted line: trastuzumab tumor uptake curve, derived from (*3*) and normalized to the day 1 and 2 SUV_{max} response threshold data (open triangles). SUV = standardized uptake value (activity concentration decay-corrected to time of injection x body weight ÷ injected activity); SUV_{max} = single-voxel maximum SUV; Resp Thld = response threshold.

SUPPLEMENTAL TABLE 1.

Methods Used to Assess Measurability and Measure Tumor Uptake (SUV_{max}) of ^{64}Cu-DOTA-trastuzumab

Alignment of tumor images among different scans*	Segmentation of ^{64}Cu tumor images†	Assessment of max voxel overlap with adjacent features	# of tumors evaluated		# of tumors measurable	
			day 1	day 2	day 1	day 2
CT, axial direction	MVBT	visual inspection	21	18	13	13
CT, axial direction + correction of PET-CT misalignment	"	"	5	3	3	1
CT, 3 dimensions	"	comparison with FDG VOI & between day 1 & day 2 images when both available	15	10	15	10
CT, 3 dimensions + correction of PET-CT misalignment	"	"	4	3	3	3
CT, 3 dimensions	projection of FDG VOI	"	5	4	3	2
CT, 3 dimensions + correction of PET-CT misalignment	"	"	3	3	1	1
		total	53	41	38	30

* Baseline ^{18}F-FDG, ^{64}Cu-DOTA-trastuzumab day 1 and day 2

† VOIs comprised multiple (i. e., 2 or 3) axial segments for 5 day 1 and 2 day 2 tumor images.

max = maximum; MVBT = maximum voxel-based thresholding; VOI = volume of interest.

SUPPLEMENTAL TABLE 2.

Number of Tumors per Patient Measured for Response to T-DM1, ^{64}Cu-DOTA-trastuzumab Uptake (SUV_{max}) and Both Response and ^{64}Cu-DOTA-trastuzumab Uptake

	Number of tumors				
		day 1		day 2	
Patient	Response	SUV_{max}	SUV_{max} & resp	SUV_{max}	SUV_{max} & resp
1	1	1	0	2	1
2*	12	10	10	8	8
3	0	4	0	2	0
4†	16	10	10	9	9
5	0	2	0	2	0
6	4	3	3	1	1
7	6	1	1	1	1
8‡	2	2	2	2	2
9	2	2	2	0	0
10	3	3	3	3	3
total	46	38	31	30	25

* Shown in Fig. 1C of the manuscript file
† Shown in Fig. 1B of the manuscript file
‡ Shown in Fig. 1A of the manuscript file
resp = response to T-DM1

SUPPLEMENTAL TABLE 3.
Patient Demographics and Clinical Characteristics

Parameter	Data*	
Age at study entry (y); median, range	54, 46-83	
ECOG performance status†	Status	No. of Patients
	0	2
	1	7
	2	1
HER2 status of distant metastasis		
IHC 3+	5 (1, 2, 6, 8, 31) ‡	
IHC 2+/FISH positive	4 (2, 4, 5, 16) ‡	
IHC 1+/FISH positive	1 (5) ‡	
Hormone status of metastatic disease		
ER and/or PR positive	6	
ER and PR negative	4	
Trastuzumab included in prior therapy		
none	3	
trastuzumab + chemotherapy for metastasis	7 (5, 6, 7, 11, 45, 117, 243) §	
Cause of treatment failure		
death	1	
toxicity	1	
disease progression	8	
	No. of Tumors (Patients)	
Tumor sites measured for ^{64}Cu-DOTA-trastuzumab uptake	day 1	day 2
bone	16 (5)	10 (2)
lymph nodes	11 (6)	9 (5)
liver	1	1
lung	5 (3)	5 (3)
chest wall mass	1	1
breast	3 (2)	3 (2)
brain	1	1

* Entries are numbers of patients unless otherwise indicated.
† At time of 1st T-DM1 administration
‡ Weeks between biopsy and injection of ^{64}Cu-DOTA-trastuzumab
§ Weeks since last trastuzumab administration
ER = estrogen receptor; FISH = fluorescence *in situ* hybridization;
IHC = immunohistochemistry; PR = progesterone receptor.